

Singular unlocking transition in the Winfree model of coupled oscillators

D. Dane Quinn*

Department of Mechanical Engineering, The University of Akron, Akron, Ohio 44325-3903, USA

Richard H. Rand and Steven H. Strogatz

Department of Theoretical and Applied Mechanics, Cornell University, Ithaca, New York 14853-1503, USA

(Received 15 December 2006; published 26 March 2007)

The Winfree model consists of a population of globally coupled phase oscillators with randomly distributed natural frequencies. As the coupling strength and the spread of natural frequencies are varied, the various stable states of the model can undergo bifurcations, nearly all of which have been characterized previously. The one exception is the unlocking transition, in which the frequency-locked state disappears abruptly as the spread of natural frequencies exceeds a critical width. Viewed as a function of the coupling strength, this critical width defines a bifurcation curve in parameter space. For the special case where the frequency distribution is uniform, earlier work had uncovered a puzzling singularity in this bifurcation curve. Here we seek to understand what causes the singularity. Using the Poincaré-Lindstedt method of perturbation theory, we analyze the locked state and its associated unlocking transition, first for an arbitrary distribution of natural frequencies, and then for discrete systems of N oscillators. We confirm that the bifurcation curve becomes singular for a continuum uniform distribution, yet find that it remains well behaved for any finite N , suggesting that the continuum limit is responsible for the singularity.

DOI: [10.1103/PhysRevE.75.036218](https://doi.org/10.1103/PhysRevE.75.036218)

PACS number(s): 05.45.Xt, 45.10.Hj, 89.75.Kd

I. INTRODUCTION

Spontaneous synchronization of oscillators occurs throughout the natural world, in fields ranging from physics and engineering, to biology and even human group behavior [1–6]. Examples include the synchronization of arrays of lasers [7,8], pendulums [9], Josephson junctions [10,11], and nanomechanical oscillators [12,13]; the rhythmic flashing of firefly congregations [14] and the chorusing of crickets [15,16]; the coordinated firing of neurons or cardiac pacemaker cells [17–26]; oscillatory glycolysis in yeast cell suspensions [27]; menstrual synchrony among women roommates or close friends [28,29]; synchronous applause of concert audiences [30]; and the inadvertent walking in step by the opening day crowd on London’s Millennium Bridge [31].

The theoretical study of self-synchronizing systems was pioneered by Winfree 40 years ago [1]. He considered a population of $N \gg 1$ self-sustained oscillators, with natural frequencies chosen at random from some prescribed probability distribution. Specifically, the Winfree model is

$$\dot{\theta}_i = \omega_i + \frac{\kappa}{N} \sum_{j=1}^N X(\theta_j) Z(\theta_i), \quad (1)$$

for $i=1, \dots, N$. Here $\theta_i(t)$ is the phase of the i th oscillator at time t , $\kappa \geq 0$ is the coupling strength, and the frequencies ω_i are drawn from a symmetric, unimodal density $g(\omega)$. We assume that the mean of $g(\omega)$ equals 1, by a suitable rescaling of time. The width of $g(\omega)$ is characterized by a parameter Γ . The coupling in Eq. (1) has the following interpretation: the j th oscillator exerts its effects through a phase-

dependent influence function $X(\theta_j)$; in turn, the i th oscillator responds to the mean field (the average influence of the whole population) according to a sensitivity function $Z(\theta_i)$.

Winfree found that the onset of synchronization was a threshold phenomenon, analogous to a phase transition. In the absence of coupling ($\kappa=0$), the oscillators behaved incoherently because of the dispersion of their intrinsic frequencies. Incoherence persisted as the coupling was gradually increased, until a critical coupling strength was reached. Then, suddenly, some of the oscillators began to synchronize and run at the same frequency.

In 1975 Kuramoto [32] reformulated and simplified Winfree’s model and, in a mathematical tour de force, showed how to calculate the coupling at the onset of synchronization, where the first oscillators begin to lock their rhythms together. Kuramoto’s model is

$$\dot{\theta}_i = \omega_i + \frac{K}{N} \sum_{j=1}^N \sin(\theta_j - \theta_i), \quad (2)$$

for $i=1, \dots, N$, with the frequencies chosen at random as above. This model has turned out to be much more tractable than Winfree’s, for two reasons: the sine function is simpler than the arbitrary X and Z in Eq. (1); and more importantly, the coupling depends only on the phase difference $\theta_j - \theta_i$, not on the absolute phases θ_j and θ_i separately as in Eq. (1). This algebraic feature imparts a rotational symmetry to the Kuramoto model that makes it easier to analyze.

In 1985 Ermentrout [33] studied a second transition for Kuramoto’s model. Loosely speaking, he investigated the opposite end of the synchronization process—its culmination rather than its onset. To be more precise, for a frequency distribution with compact support, Ermentrout calculated the coupling strength at which *all* the oscillators become locked

*Electronic address: quinn@uakron.edu

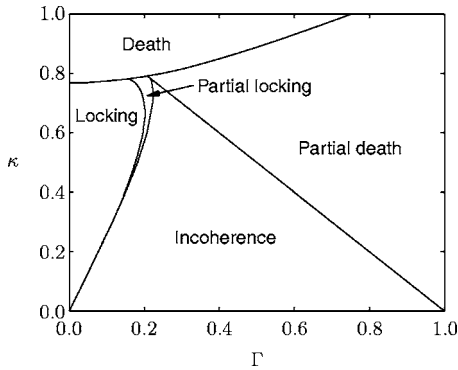


FIG. 1. Stability diagram for the Winfree model (1), with coupling strength κ and influence and sensitivity functions given by Eq. (3). The plot shows the regions of parameter space corresponding to different stable states of the system, for the case of $N=800$ oscillators with natural frequencies ω_i that are evenly spaced on the interval $[1-\Gamma, 1+\Gamma]$. This choice of frequencies approximates a uniform distribution as $N \rightarrow \infty$. The goal of this paper is to understand the perturbative properties of the curve that bounds the “locking” region. (Diagram adapted from Ref. [41].)

to the same frequency, a state known as complete frequency locking or full synchrony.

In the intervening decades, the analysis of Kuramoto’s model has generated an enormous literature [34–38], whereas Winfree’s model has been relegated to the footnotes (for reviews of the work on the Kuramoto model, see Refs. [39,40]). But a few years ago, [41] exhumed Winfree’s model in the continuum limit as $N \rightarrow \infty$ and showed that it too becomes tractable, at least for the special case where the model’s influence and sensitivity functions have just a single Fourier component, namely where

$$X(\theta) = 1 + \cos \theta, \quad Z(\theta) = -\sin \theta. \quad (3)$$

Then, in the limit of weak coupling and nearly identical natural frequencies, Winfree’s model reduces to Kuramoto’s (in the sense that one can show that the averaged or “slow time” equations for the Winfree model are isomorphic to the Kuramoto model, with coupling $K = \kappa/2$). Away from this limiting regime, the Winfree model displays collective behavior not seen in the Kuramoto model, including oscillator death and various hybrid states combining incoherent, dead, and frequency-locked oscillators.

Figure 1 shows where the various stable states lie in parameter space, for the case where the frequencies are evenly spaced in the interval $[1-\Gamma, 1+\Gamma]$. Notice that near the origin, there are just three possibilities: locking, incoherence, and a thin strip of partial locking (where some of the oscillators are locked and the others are desynchronized). These are precisely the stable states seen in the Kuramoto model—as they must be, given that the Kuramoto model governs the long-time dynamics of the Winfree model (1) and (3), in the limit where both Γ and κ are small.

Ariaratnam and Strogatz showed that all but one of the bifurcation curves in Fig. 1 could be obtained analytically. Unfortunately, the curve that could not be calculated was an important one: the boundary between locking and partial

locking. Attempts to derive this curve kept running into obstacles—the series expansions in powers of the coupling would become singular at cubic order, which seemed mysterious given that the corresponding numerics showed no hint of singular behavior.

In this paper, we try to understand why the earlier calculation broke down. The strategy is to derive the boundary of the locked state using the perturbative technique known as the Poincaré-Lindstedt method [42]. This method assumes a periodic solution of the governing equations (implying that all the oscillators are running with the same frequency, though the phase differences between them need not be zero or even constant). The period of the collective motion is unknown and is to be determined perturbatively as part of the solution.

We find that a singularity does indeed occur at cubic order in perturbation theory, and that this is due to a combination of two effects: (i) the discontinuous jumps at the endpoints of the assumed frequency distribution, and (ii) the implicit passage to a continuum (infinite- N) limit of the model. For any finite number of oscillators, no singularity arises, and the theoretical predictions match the numerical results. Furthermore, we provide strong evidence (but have been frustratingly unable to prove) that the order of divergence in the singularity is precisely what one would expect, when integrals are replaced by the corresponding finite- N sums. The conclusion is that the continuum limit of the model is more subtle than one might have imagined.

As the discussion above should suggest, our work in this paper is motivated principally by mathematical considerations, not scientific ones. We regard the Winfree model as a fascinating dynamical system with a life of its own, worthy of study in its own right. At the same time we recognize the importance of connecting it to the real-world phenomena that originally inspired it. In the past few years there have been some encouraging advances in this direction [43]. For example, the emergence of synchronization in a system of coupled electrochemical oscillators has been shown to agree quantitatively with the predictions of the Kuramoto model [44], and the influence and sensitivity functions of real neurons have recently been measured for the first time [23], thus paving the way for an analysis of coupled neural systems in these terms. But, to be candid, we doubt that the results presented here will have similar experimental impact. The theoretical subtleties of the infinite- N limit are unlikely to have salient testable consequences, precisely because of our result that the finite- N system is well behaved for all N . Moreover, we still do not know which features of the model are responsible for the singularity, so we cannot say how generic our results would be for real systems of coupled oscillators. The reader should take these admissions for what they are: an invitation to help resolve the mathematical questions that remain. Several suggestions for such research are indicated in the final section.

II. MODEL

As in Ariaratnam and Strogatz [41] we consider the special case of the Winfree model given by the following integro-differential equation:

$$\frac{\partial \Theta}{\partial t}(t, \nu) = 1 + \Gamma \nu - \kappa \sin \Theta(t, \nu) \int_{-1}^1 [1 + \cos \Theta(t, \mu)] h(\mu) d\mu, \quad (4)$$

for all $-1 \leq \nu \leq 1$. Here $\Theta(t, \nu)$ denotes the phase at time t of an oscillator with natural frequency $1 + \Gamma \nu$. Note that by a choice of time scale, the mean natural frequency across the population has been set to unity, without loss of generality. The parameter $\Gamma > 0$ represents the width of the frequency distribution, and $-1 \leq \nu \leq 1$ is a normalized detuning, a measure of how far an oscillator's natural frequency deviates from the population mean. The expression containing the integral represents global coupling to all the other oscillators in the population. The prefactor $\kappa > 0$ is the coupling strength. The sensitivity function $Z[\Theta(t, \nu)] = -\sin \Theta(t, \nu)$ quantifies how the given oscillator changes its instantaneous frequency in response to the collective influence of all the others. Within the integral, the term $X[\Theta(t, \mu)] = 1 + \cos \Theta(t, \mu)$ describes the influence of an oscillator, with detuning μ , on the given oscillator with detuning ν . These influences are expressed with a weight $h(\mu)$, the probability density of natural frequencies (more precisely, the probability density of normalized detunings) across the population. For simplicity, we assume $h(\mu)$ is an even function subject to the normalization condition

$$\int_{-1}^1 h(\mu) d\mu = 1. \quad (5)$$

The formulation above allows us to handle both discrete and continuous distributions of natural frequencies in a single framework. For example, to represent the discrete case where the oscillators have detunings ν_i , for $i=1, \dots, N$, we can write

$$h(\nu) = \frac{1}{N} \sum_{i=1}^N \delta(\nu - \nu_i). \quad (6)$$

Then the integro-differential equation (4) reduces to the set of N ordinary differential equations given by Eqs. (1) and (3).

III. PERTURBATION THEORY

To analyze Eq. (4) with perturbation theory, we assume that the parameters κ and Γ are small, corresponding to a system of weakly coupled, nearly identical oscillators. Taking the coupling as a small parameter $0 < \epsilon \ll 1$, we set $\kappa = \epsilon$ and replace Γ by $\epsilon \Gamma$ from now on.

In effect, we are considering the joint limit in which both the coupling strength κ and the frequency spread Γ tend to zero simultaneously along some curve in parameter space. That is the appropriate limit for this problem, as evidenced by the shape of the numerically computed bifurcation curve for the unlocking transition. As shown in Fig. 1, the unlocking curve emanates from the origin with a nonzero slope, indicating that we need to consider the joint limit. In contrast, if we were to allow one parameter to become small while holding the other fixed, we would not see any transi-

tion or interesting dynamics. The system would either act uncoupled (and hence incoherent), or would have identical oscillators (and hence would synchronize perfectly, with all oscillators in phase).

Our approach uses the Poincaré-Lindstedt method [42] to characterize periodic solutions for $\epsilon \neq 0$ and to identify the bifurcation curve on which these periodic solutions disappear. Any such periodic solution can be written in the following ansatz:

$$\Theta(t, \nu, \epsilon) = \Omega(\epsilon)t + \Phi(\nu, \epsilon) + \hat{\Theta}(t, \nu, \epsilon). \quad (7)$$

Here $\Omega(\epsilon)$ represents the collective locked frequency of the population [where $\Omega(\epsilon)$ is to be determined in the course of the analysis], and $\Phi(\nu, \epsilon) + \hat{\Theta}(t, \nu, \epsilon)$ describes the phase evolution of each oscillator with respect to a frame rotating at the locked frequency. The time-independent phase offset $\Phi(\nu, \epsilon)$ is defined such that the remaining oscillatory term has zero mean over one cycle,

$$\int_0^{2\pi/\Omega} \hat{\Theta}(t, \nu, \epsilon) dt = 0. \quad (8)$$

From now on, time is nondimensionalized as $\tau = \Omega(\epsilon)t$, and we expand everything in the form of the following regular perturbation series:

$$\begin{aligned} \epsilon \Gamma &= \sum_{i=1}^{\infty} \epsilon^i \gamma_i, & \Omega(\epsilon) &= 1 + \sum_{i=1}^{\infty} \epsilon^i \omega_i, \\ \hat{\Theta}(\tau, \nu, \epsilon) &= \sum_{i=1}^{\infty} \epsilon^i \theta_i(\tau, \nu), & \Phi(\nu, \epsilon) &= \sum_{i=0}^{\infty} \epsilon^i \phi_i(\nu). \end{aligned} \quad (9)$$

Substitution of these series into Eq. (4) yields the following equation at $O(\epsilon)$:

$$\begin{aligned} \frac{\partial \theta_1}{\partial \tau}(\tau, \nu) &= -\omega_1 + \gamma_1 \nu - \sin[\tau + \phi_0(\nu)] \int_{-1}^1 \{1 + \cos[\tau \\ &+ \phi_0(\mu)]\} h(\mu) d\mu. \end{aligned} \quad (10)$$

At $O(\epsilon^2)$ and $O(\epsilon^3)$ the equations of motion, although straightforward, are lengthy and are omitted for brevity.

In the course of working through the analysis at successively higher orders, we noticed that certain quantities kept reappearing, and it therefore proves convenient to introduce a compact notation for them at the outset. These quantities have to do with the series expansion of the global coupling term in powers of ϵ . Specifically, the μ average of $\exp[i\Phi(\mu, \epsilon)]$ generates terms that enter at each order of perturbation theory. This motivates the following definitions.

Let angle brackets denote an average over the population:

$$\langle e^{i\Phi} \rangle = \int_{-1}^1 e^{i\Phi(\mu, \epsilon)} h(\mu) d\mu. \quad (11)$$

If we expand this average in powers of ϵ , we obtain

$$\langle e^{i\Phi} \rangle = \sum_{j=0}^{\infty} \epsilon^j r_j e^{i\psi_j}, \quad (12)$$

where r_j and ψ_j denote the magnitude and argument of the complex coefficient of ϵ^j in the Maclaurin series. Equivalently, the complex coefficients have real and imaginary parts given by

$$r_j \cos \psi_j = \left. \frac{1}{j!} \frac{d^j}{d\epsilon^j} \langle \cos \Phi \rangle \right|_{\epsilon=0}, \quad (13a)$$

$$r_j \sin \psi_j = \left. \frac{1}{j!} \frac{d^j}{d\epsilon^j} \langle \sin \Phi \rangle \right|_{\epsilon=0}. \quad (13b)$$

These can be combined to yield

$$r_j = \left. \frac{1}{j!} \frac{d^j}{d\epsilon^j} (\langle \cos \Phi \rangle \cos \psi_j + \langle \sin \Phi \rangle \sin \psi_j) \right|_{\epsilon=0}, \quad (14a)$$

$$0 = \left. \frac{1}{j!} \frac{d^j}{d\epsilon^j} (\langle \cos \Phi \rangle \sin \psi_j - \langle \sin \Phi \rangle \cos \psi_j) \right|_{\epsilon=0}. \quad (14b)$$

The series $R = \sum \epsilon^j r_j$ turns out to be the counterpart of the order parameter in Kuramoto's model [3,39]. Moreover, just as in Kuramoto's classic analysis, the presence of this order parameter suggests a solution strategy based on a self-consistency argument. Roughly speaking, at each order of perturbation theory, the relevant differential equation and its solution will be found to depend on some particular r_j and ψ_j as parameters; but then that solution must also be consistent with the equations that defined r_j and ψ_j in the first place. In this way, the requirement for self-consistency implies algebraic conditions that help determine the unknown coefficients in the solution.

For instance, the $O(\epsilon)$ equation (10) can be rewritten in a way that incorporates r_0 and ψ_0 as

$$\frac{\partial \theta_1}{\partial \tau}(\tau, \nu) = -\omega_1 + \gamma_1 \nu - \sin[\tau + \phi_0(\nu)][1 + r_0 \cos(\tau + \psi_0)]. \quad (15)$$

To make further headway, we recall that the oscillatory terms $\theta_i(\tau, \nu)$ are 2π -periodic in τ and have zero mean over one cycle, according to their definition. Thus, in the differential equation for θ_1 above, we must get zero if we integrate the right-hand side over one cycle. Imposing this condition (equivalent to removing secular terms) yields

$$0 = -\omega_1 + \gamma_1 \nu - \frac{r_0}{2} \sin[\phi_0(\nu) - \psi_0]. \quad (16)$$

Now we invoke the self-consistency conditions (14). For $j=0$ these reduce to

$$r_0 = \int_{-1}^1 \cos[\phi_0(\mu) - \psi_0] h(\mu) d\mu, \quad (17a)$$

$$0 = \int_{-1}^1 \sin[\phi_0(\mu) - \psi_0] h(\mu) d\mu. \quad (17b)$$

Solving Eq. (16) for $\sin[\phi_0(\nu) - \psi_0]$ and making use of the second of the self-consistency conditions (17) and the assumed evenness of $h(\mu)$, one finds that

$$\omega_1 = 0. \quad (18)$$

Next, without loss of generality we can set

$$\psi_0 = 0, \quad (19)$$

since Eqs. (7) and (14) show that this can always be achieved by shifting the origin of time, $t \rightarrow t - t_0$ for a suitable t_0 , if necessary. With this choice of ψ_0 , the phase offset satisfies $\phi_0(-1) = -\phi_0(1)$, and the solvability condition (16) becomes

$$\frac{2\gamma_1}{r_0} \nu = \sin[\phi_0(\nu)]. \quad (20)$$

The value of r_0 must still be found in a self-consistent manner from Eq. (17) so that

$$r_0 = \int_{-1}^1 \cos[\phi_0(\mu)] h(\mu) d\mu. \quad (21)$$

Thus the problem reduces to solving Eqs. (20) and (21) simultaneously for the unknowns r_0 and $\phi_0(\nu)$. This problem has already been studied and solved; it arises in the analysis of the Kuramoto model.

At this point it becomes crucial to distinguish between finite and infinite populations of oscillators, because the previous work on the Kuramoto model has shown that their bifurcation behavior is different. Imagine that we start with a stable locked state and slowly increase the width Γ of the natural frequency distribution. For the finite- N case [45,46], the stable locked state is lost at a saddle-node bifurcation, and this is known to occur when the maximum phase offset $\phi_0(1)$ is close to, but strictly less than, $\pi/2$. In contrast, for the infinite- N case [33] there is no saddle-node bifurcation, at least not when the frequency distribution is even and unimodal; instead, locking is lost when the maximum phase $\phi_0(1) = \pi/2$. Since in this paper we are concerned with the limiting behavior of the finite- N system, we will henceforth impose the saddle-node condition at the unlocking transition. Also, keep in mind that although the density $h(\mu)$ may look like it represents a continuous distribution in the formulas below, it actually represents a discrete system, via the device in Eq. (6).

Let us now return to the analysis of Eqs. (20) and (21), to see how a saddle-node bifurcation arises when N is finite. Changing variables from μ to ϕ_0 yields

$$2\gamma_1 = \int_{-\phi_0(1)}^{\phi_0(1)} \cos^2(\phi_0) h \left(\frac{\sin(\phi_0)}{\sin[\phi_0(1)]} \right) d\phi_0, \quad (22)$$

which can be solved for $\phi_0(1)$, if and only if the saddle-node bifurcation has not yet occurred (Fig. 2).

The right-hand side of Eq. (22) is a function of $\phi_0(1)$. At the saddle-node bifurcation the derivative of this function with respect to $\phi_0(1)$ vanishes. With some manipulation the

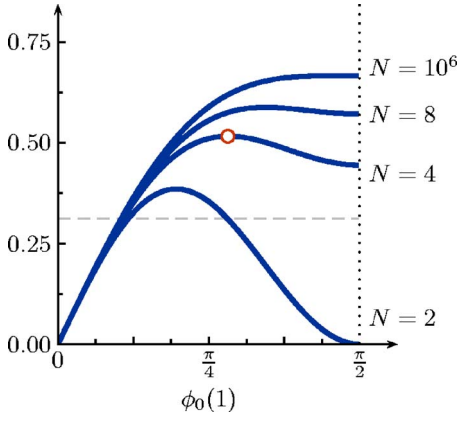


FIG. 2. (Color online) Graphical solution to Eq. (22), the self-consistency condition, for discrete populations. The curves show graphs of the right-hand side of Eq. (22) for four different population sizes N . In the example shown, the detunings were chosen according to a discrete uniform distribution given by Eqs. (6) and (38). The horizontal dashed line represents the left-hand side of Eq. (22), a constant function of height $2\gamma_1$. Intersections between the dashed line and the curve correspond to locked states (solutions of the self-consistency equation), and determine the value of the maximum phase offset $\phi_0(1)$ for such a state. Notice that for typical values of γ_1 there are two intersections for each N , indicating that there are two locked states (presumably one stable, and the other unstable). As γ_1 increases, these states approach each other and collide in a saddle-node bifurcation at the local maximum of the curve. Above this point, no locked solutions exist. The point marked by a small open circle corresponds to a saddle-node bifurcation for $N=4$, at $[\gamma_1^*, \phi_0^*(1)] = (0.884, 0.516)$. As N increases, the saddle-node value of $\phi_0^*(1)$ moves to the right and ultimately tends to $\pi/2$ as $N \rightarrow \infty$.

zero-derivative condition for the saddle-node bifurcation can be rewritten as

$$r_0 = \int_{-1}^1 \frac{\sin^2[\phi_0(\mu)]}{\cos[\phi_0(\mu)]} h(\mu) d\mu, \quad (23)$$

a result that has also been obtained by other arguments [45,46]. Combining this with Eq. (22), we find that the location of the saddle-node bifurcation is determined from the solution of the equation

$$0 = \int_{-1}^1 \frac{\cos[2\phi_0(\mu)]}{\cos[\phi_0(\mu)]} h(\mu) d\mu. \quad (24)$$

This can be written as

$$0 = \int_{-\phi_0^*(1)}^{\phi_0^*(1)} \cos(2\phi_0) h\left(\frac{\sin(\phi_0)}{\sin[\phi_0^*(1)]}\right) d\phi_0, \quad (25)$$

where $\phi_0^*(1)$ corresponds to the maximum phase offset at the bifurcation. By using the cosine double-angle formula in Eq. (24) and invoking Eq. (20), we find that the value of γ_1 at the bifurcation is given by

$$\gamma_1^* = \frac{\sin[\phi_0^*(1)]}{4} \int_{-1}^1 \frac{h(\mu)}{\cos[\phi_0(\mu)]} d\mu. \quad (26)$$

At higher orders of perturbation theory, the strategy is much the same. Omitting the details, we find that at $O(\epsilon^2)$, the solvability condition (for removal of secular terms) can be expressed as

$$0 = -\omega_2 + \gamma_2 \nu - \frac{1}{2} \left[\left(1 + \frac{r_0^2}{8} \right) + \frac{r_0}{8} \cos[\phi_0(\nu)] \right] - \frac{1}{2} \{ r_1 \sin[\phi_0(\nu) - \psi_1] + r_0 \phi_1(\nu) \cos[\phi_0(\nu)] \}. \quad (27)$$

The self-consistency conditions for $j=1$ become

$$r_1 = - \int_{-1}^1 \phi_1(\mu) \sin[\phi_0(\mu) - \psi_1] h(\mu) d\mu, \quad (28a)$$

$$0 = - \int_{-1}^1 \phi_1(\mu) \sin[\phi_0(\mu) - \psi_1] h(\mu) d\mu, \quad (28b)$$

which imply that

$$\omega_2 = -\frac{1}{2} \left(1 + \frac{r_0^2}{4} \right), \quad \psi_1 = \frac{\pi}{2}. \quad (29)$$

Imposing the saddle-node bifurcation yields $r_0 \gamma_2^* / \gamma_1^* = 0$ and hence

$$\gamma_2^* = 0. \quad (30)$$

Next, from the $O(\epsilon^3)$ solvability condition (not shown), the self-consistency conditions for $j=2$ yield

$$\omega_3 = 0, \quad (31)$$

and at the saddle-node bifurcation,

$$0 = -r_0 \frac{\gamma_3^*}{\gamma_1^*} - \frac{r_0}{64} \left[17 + \left(\int_{-1}^1 \cos[2\phi_0(\mu)] h(\mu) d\mu \right)^2 \right] + \frac{r_0}{64} \left(1 - \frac{r_0}{2} \int_{-1}^1 \frac{1}{\cos^3[\phi_0(\mu)]} h(\mu) d\mu \right). \quad (32)$$

Finally this brings us to the puzzling result that motivated this paper: the cubic coefficient of Γ on the bifurcation curve satisfies

$$\gamma_3^* = -\frac{\gamma_1^*}{64} \left[16 + \left(\int_{-1}^1 \cos[2\phi_0(\mu)] h(\mu) d\mu \right)^2 + \left(\frac{r_0}{2} \int_{-1}^1 \frac{1}{\cos^3[\phi_0(\mu)]} h(\mu) d\mu \right) \right], \quad (33)$$

and this expression can become singular, as we will now show.

IV. CALCULATING THE COEFFICIENTS

A. Uniform distribution

For a continuous uniform distribution of natural frequencies [$h(\nu) = 1/2$], the maximum phase offset at the unlocking transition is given by $\phi_0^*(1) = \pi/2$, as proven by Ermentrout

and as mentioned above. Hence, substitution of $\nu=1$ into Eq. (20) yields $2\gamma_1^*/r_0=1$ and thus

$$\sin[\phi_0(\nu)] = \nu. \quad (34)$$

These results, together with the self-consistency condition (21), then imply that

$$\gamma_1^* = \frac{\pi}{8}, \quad (35)$$

$$r_0 = \frac{\pi}{4}. \quad (36)$$

As ν ranges from -1 to 1 , the corresponding phases ϕ_0 cover the entire interval $[-\pi/2, \pi/2]$. So when Eq. (33) is evaluated to determine γ_3^* , the integral

$$\int_{-1}^1 \frac{1}{\cos^3[\phi_0(\mu)]} h(\mu) d\mu \quad (37)$$

blows up because of the singularities at the endpoints, and therefore the cubic coefficient of Γ diverges.

However, in Ariaratnam and Strogatz [41] numerical results were presented for 800 oscillators with evenly spaced frequencies (approximating the uniform distribution), and the location of the bifurcation curve was identified in terms of the parameters. Surprisingly, there was no indication of any singularity in the bifurcation curve.

B. Discrete uniform population

Now consider a discrete population of N oscillators with evenly spaced frequencies, for which the distribution function $h(\nu)$ can be written as a sum of delta functions,

$$h(\nu) = \frac{1}{N} \sum_{i=1}^N \delta \left[\nu - \left(1 - 2 \frac{i-1}{N-1} \right) \right]. \quad (38)$$

In the limit $N \rightarrow \infty$, this approaches a uniform distribution with $h(\nu) = 1/2$.

However, since N is now finite, the maximum phase offset at the unlocking transition is no longer simply $\phi_0^*(1) = \pi/2$. Instead, $\phi_0^*(1)$ is implicitly determined by the saddle-node bifurcation condition. Furthermore, the value of $\phi_0^*(1)$ will depend on N .

For the discrete uniform population considered here, the saddle-node condition (25) can be rewritten (again using the cosine double-angle formula) as

$$0 = \sum_{i=1}^N \left(2 \left\{ 1 - \left[\sin[\phi_0^*(1)] \left(1 - 2 \frac{i-1}{N-1} \right) \right]^2 \right\}^{1/2} - \left\{ 1 - \left[\sin[\phi_0^*(1)] \left(1 - 2 \frac{i-1}{N-1} \right) \right]^2 \right\}^{-1/2} \right). \quad (39)$$

This equation determines $\sin[\phi_0^*(1)]$ implicitly as a function of N . We solved it numerically, using a bracketing method in MATLAB with double precision variables to ensure an accurate solution for large N .

Figure 3(a) shows the results of such computations. The numerics suggest that as $N \rightarrow \infty$,

$$\sin[\phi_0^*(1)] \sim 1 - cN^{-1}, \quad (40)$$

where

$$c \approx 0.605\,443\,657 \dots, \quad (41)$$

as obtained by root-finding supplemented by Richardson extrapolation. Hence

$$\phi_0^*(1) \sim \frac{\pi}{2} - \sqrt{2c}N^{-1/2}. \quad (42)$$

We would love to be able to derive an analytical expression for c in the asymptotic expansion (40), but so far we have been stymied. Approximating the Riemann sums in Eq. (34) by integrals and then solving for $\sin[\phi_0^*(1)]$ immediately yields the constant term, $\sin[\phi_0^*(1)] \sim 1$, but how does one find a formula for c in the correction term? We have tried using the trapezoid rule and its generalization, the Euler-Maclaurin summation formula, to approximate the sums in Eq. (39) asymptotically for large N , but analysis along these lines does not produce a formula for c that matches the numerics. The trouble is that the asymptotics are delicate [47,48]. The Euler-Maclaurin formula works well over a large range of $\sin[\phi_0^*(1)]$, but it begins to diverge just in the region where we need to apply it. The source of the difficulty is that one of the sums in Eq. (39) has an integrable singularity at $\sin[\phi_0^*(1)]=1$, while at the same time, the desired root (40) approaches this singularity as $N \rightarrow \infty$.

In any case, once $\sin[\phi_0^*(1)]$ has been computed, the value of $\phi_0^*(1)$ can then be used to compute γ_1^* from Eq. (26) and γ_3^* from Eq. (33). Because the frequency distribution is discrete (a sum of delta functions), the integrals for γ_1^* and γ_3^* also become finite sums. To evaluate the various cosine terms in the sums (26) and (33), we also need to make use of Eq. (20) when the saddle-node condition is imposed. Then the oscillator phases satisfy

$$\sin[\phi_0(\nu)] = a\nu, \quad (43)$$

where

$$a = \sin[\phi_0^*(1)]. \quad (44)$$

Figure 3(b) shows that as N increases, the resulting γ_1^* approaches a limiting value. This limit equals $\pi/8$, just as expected from Eq. (35).

In contrast, the magnitude of γ_3^* appears to increase without bound, as illustrated in Figs. 3(c) and 3(d). Notice that the growth starts slowly: at $N=10^6$, Eq. (33) evaluates to $\gamma_3^* \approx -5.0$. We now seek to understand this interesting behavior of γ_3^* .

C. Asymptotic behavior of γ_3^*

Assuming that the value of $1 - \sin[\phi_0^*(1)]$ scales as conjectured above, like N^{-1} as $N \rightarrow \infty$, we can show that γ_3^* scales as a square root, $\gamma_3^* \sim bN^{1/2}$ as $N \rightarrow \infty$. The numerical results of Fig. 3(d) agree with this scaling and indicate that the prefactor $b \approx -0.005$.

To derive this scaling law for γ_3^* , consider the finite sum corresponding to the integral (37). Using the discretization (38) we obtain

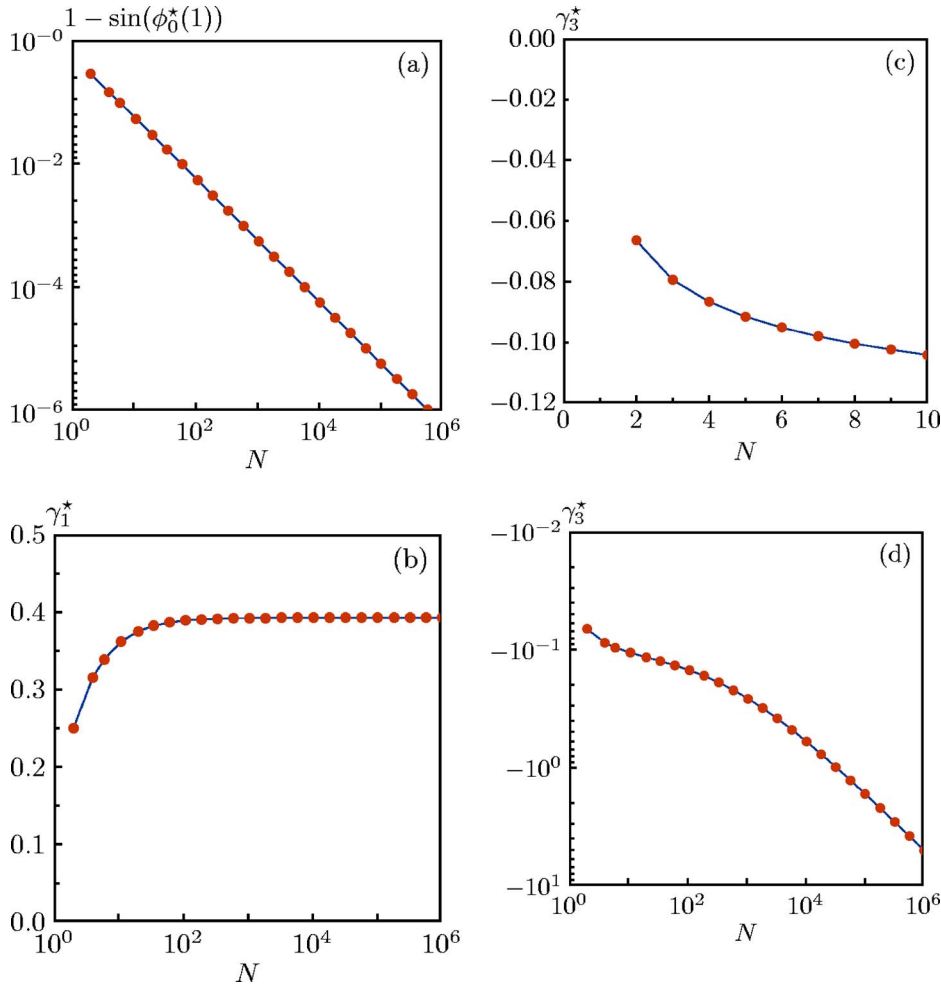


FIG. 3. (Color online) Scaling laws for the discrete uniform distribution. (a) The maximum phase offset satisfies $1 - \sin[\phi_0^*(1)] \sim cN^{-1}$, with c given by Eq. (41). (b) The linear coefficient γ_1^* converges to $\pi/8$ for large N , as expected from the continuum limit (35). (c) The cubic coefficient γ_3^* is small and slowly becomes more negative for small values of N . (d) As N increases, γ_3^* remains moderately small and negative, but eventually diverges according to the square-root scaling law (57).

$$\int_{-1}^1 \frac{1}{\cos^3[\phi_0(\nu)]} h(\nu) d\nu = \frac{1}{N} S(N, a), \quad (45)$$

where

$$S(N, a) = \sum_{i=1}^N f(\nu_i), \quad (46)$$

$$f(\nu) = (1 - a^2 \nu^2)^{-3/2}, \quad (47)$$

and

$$\nu_i = 1 - 2 \frac{i-1}{N-1}. \quad (48)$$

Although we cannot evaluate $S(N, a)$ in closed form, we can write down upper and lower bounds on it. The idea is to use numerical quadrature rules in reverse. The sum is closely related to the rectangular and trapezoidal approximations for $\int_{-1}^1 f(\nu) d\nu$; by exploiting the concavity of f , we can turn these approximations into rigorous bounds.

For example, because the graph of f is concave up, the area beneath it is strictly less than that given by the trapezoid rule. Hence

$$\int_{-1}^1 f(\nu) d\nu < \frac{2}{N-1} \left(\frac{1}{2} f(\nu_1) + \sum_{i=2}^{N-1} f(\nu_i) + \frac{1}{2} f(\nu_N) \right). \quad (49)$$

The expression in parentheses is almost $S(N, a)$, except that the endpoint terms contain factors of $1/2$. To compensate for this, we manually add $(1/2)[f(\nu_1) + f(\nu_N)] = f(1)$ inside the parentheses and balance this by adding the resulting term $2f(1)/(N-1)$ to the other side of the inequality. Thus we arrive at a lower bound on S ,

$$S(N, a) > f(1) + \frac{N-1}{2} \int_{-1}^1 f(\nu) d\nu. \quad (50)$$

After carrying out the integral this reduces to

$$S(N, a) > \frac{1}{(1-a^2)^{3/2}} + \frac{N-1}{\sqrt{1-a^2}}. \quad (51)$$

Similarly, we can use lower rectangles to obtain a lower bound on the integral, which then yields an upper bound on the sum. The result is

$$S(N, a) < 2f(1) - f(0) + \frac{N-1}{2} \int_{-1}^1 f(\nu) d\nu, \quad (52)$$

which simplifies to

$$S(N, a) < \frac{2}{(1-a^2)^{3/2}} - 1 + \frac{N-1}{\sqrt{1-a^2}}. \quad (53)$$

These bounds are valid for any fixed $N > 1$ and fixed $0 < a < 1$. But since we are primarily interested in the large- N limit of the sum, we now substitute $a \sim 1 - c/N$, as suggested by the observed scaling law (40), and examine the asymptotic behavior of the bounds as $N \rightarrow \infty$. To leading order, we find

$$\frac{1+2c}{2\sqrt{2}c^{3/2}} N^{3/2} < S(N, 1-c/N) < \frac{1+c}{\sqrt{2}c^{3/2}} N^{3/2}. \quad (54)$$

For c given by (41) these bounds imply that $1.66N^{3/2} < S < 2.41N^{3/2}$ for large N . In fact, using direct computation supplemented by Richardson extrapolation, we find that

$$\lim_{N \rightarrow \infty} \frac{S(N, 1-c/N)}{N^{3/2}} = 2.038\,169\dots, \quad (55)$$

which is consistent with our bounds. Unfortunately we have not been able to evaluate this limit in closed form, or even to prove that it exists. (The usual convergence tests do not apply.)

Nevertheless, Eqs. (54) and (55) suffice to explain why γ_3^* grows like \sqrt{N} . The dominant contribution to γ_3^* in Eq. (33) is

$$-\frac{\gamma_1^*}{64} \left(\frac{r_0}{2} \int_{-1}^1 \frac{1}{\cos^3[\phi_0(\mu)]} h(\mu) d\mu \right). \quad (56)$$

After substituting $\gamma_1^* = \pi/8$, $r_0 = \pi/4$, and making use of Eqs. (45) and (55), we find

$$\gamma_3^* \sim \frac{-\pi^2}{4096} (2.038\,169\dots) \sqrt{N}, \quad (57)$$

which reduces to $\gamma_3^* \sim (-0.004\,91\dots) \sqrt{N}$, thus accounting for the scaling law seen numerically in Fig. 3(d). The smallness of the prefactor here explains why γ_3^* is unnoticeable for small systems of oscillators, and why it has only reached a value of roughly -5 for systems of a million oscillators.

D. Even polynomial distributions

One might wonder whether the divergences seen above are artifacts of the uniform frequency distribution we have been assuming. In related problems [33,46], it is known that the uniform case is nongeneric in certain respects, compared to other unimodal distributions with even symmetry. To shed light on this issue, we now consider a broader class of such distributions, first for the continuous case and then for the discrete. We will see that the divergences persist, though with different scaling laws.

For an even polynomial distribution of frequencies, the density can be expressed as

$$h(\nu) = \sum_{k=0}^{\infty} h_k |\nu|^k. \quad (58)$$

Then the saddle-node bifurcation condition becomes

$$\begin{aligned} 0 &= \int_{-1}^1 \frac{\cos[2\phi_0(\mu)]}{\cos[\phi_0(\mu)]} \sum_{k=0}^{\infty} h_k |\mu|^k d\mu \\ &= \sum_{k=0}^{\infty} \frac{2h_k}{\sin^k[\phi_0(1)]} \int_0^{\phi_0^*(1)} \cos(2\phi_0) \sin^k(\phi_0) d\phi_0. \end{aligned} \quad (59)$$

In particular, consider a piecewise linear distribution of the form

$$h(\nu) = h_0 + (1-2h_0)|\nu|. \quad (60)$$

For $h_0=1$ this can be described as a tent-shaped distribution, while for $h_0=1/2$ it reduces to the uniform distribution considered above. With this, the condition for the saddle-node bifurcation reduces to

$$0 = \left(\frac{h_0-2}{3} \right) \cos^3[\phi_0^*(1)] + (1-h_0) \cos[\phi_0^*(1)] - \left(\frac{1-2h_0}{3} \right). \quad (61)$$

One solution to this equation is $\cos[\phi_0^*(1)]=1$, while the remaining solutions satisfy the equation

$$0 = \cos^2[\phi_0^*(1)] + \cos[\phi_0^*(1)] + \left(\frac{2h_0-1}{2-h_0} \right), \quad (62)$$

so that

$$\cos[\phi_0^*(1)] = -\frac{1}{2} \pm \sqrt{\frac{6-9h_0}{4(2-h_0)}}. \quad (63)$$

Therefore, for $h_0=1/2$ the maximum phase offset at the bifurcation is $\phi_0^*(1)=\pi/2$. In addition, for $h_0 > 1/2$ no solution for $\phi_0^*(1)$ exists so that no saddle-node bifurcation is found for this system. This confirms what we already knew on general theoretical grounds, namely, that saddle-node bifurcations do not occur for continuous, even, unimodal frequency distributions [33]. Instead, locking is lost when the $O(\epsilon)$ phase distribution covers the interval $-\pi/2 \leq \phi_0(\nu) \leq \pi/2$.

E. Discrete piecewise linear distribution

Now we ask what happens in the discrete case, where saddle-node bifurcations become possible again. The family of piecewise linear distributions considered above have a discrete counterpart, in which

$$h(\nu) = \frac{2}{N} \sum_{i=1}^N [h_0 + (1-2h_0)|\nu|] \times \delta \left[\nu - \left(1 - 2 \frac{i-1}{N-1} \right) \right]. \quad (64)$$

As for the discrete uniform population, the condition for the saddle-node bifurcation reduces to a nonlinear algebraic equation that can be solved for $\phi_0^*(1)$ with MATLAB. This value can then be used to determine the bifurcation curve from Eqs. (26) and (33).

Figure 4 shows that as N increases, the quantities $\phi_0^*(1)$ and γ_1^* approach stationary values; beyond $N \geq 10^3$ little variation is observed. In contrast, the value of γ_3^* along the bifurcation curve does not converge as N increases. Instead the magnitude of this term appears to grow as N^2 . This is a much more rapid divergence than the $N^{1/2}$ behavior seen for the uniform case. Hence we conclude that the divergence of γ_3^* is not an artifact of a uniform distribution. Indeed, the divergence becomes even more severe when the distribution is tentlike.

V. OPEN QUESTIONS

We are still confused about several questions that arose in our analysis, and would welcome insights from our colleagues.

First, can any of the scaling laws found here be derived more convincingly? We keep feeling that these should be tractable calculations, and hope that experts in asymptotics will look into them. For example, what equation determines the coefficient c in Eq. (40)? Can the other scaling laws (for the large- N dependence of γ_1^* and γ_3^*) be shown to follow directly from this first one, not just in the sense of bounds but with genuine asymptotics?

Second, what are the implications of the singular behavior found in the bifurcation curve at the unlocking transition? Should one infer that the assumed form of the curve, given by the regular perturbation series $\epsilon\Gamma = \sum_{i=1}^{\infty} \epsilon^i \gamma_i$, is valid for all finite N but wrong in the continuum limit? If so, that would suggest that the bifurcation curve loses a certain amount of differentiability (since the singularity occurs only in the cubic coefficient, and not in the linear one). But then what is the correct form of the bifurcation curve in this case? In other words, what is the precise algebraic nature of the singularity?

Third, how generic is the singularity found here? We can see that it stems from the $1/\cos^3[\phi_0(\mu)]$ term in the integrand of Eq. (33). Would it still occur if the influence and sensitivity functions were generic periodic functions containing all harmonics in their Fourier series? Or is it an artifact of our tractable special case, where only first harmonics were allowed?

Fourth, how do these results depend on the nature of the assumed frequency distribution? The presence of even stronger singular behavior for the tentlike frequency distributions hints that the unlocking transition may display singular behavior for *any* unimodal distribution with compact support, in the continuum limit. If this is true, what are the dynamical consequences, if any, for the Winfree model? For the past 40 years, much of the research on populations of coupled oscillators has taken a cavalier approach to the infinite- N limit, and no major problems have arisen. Are we now starting to see some subtleties here?

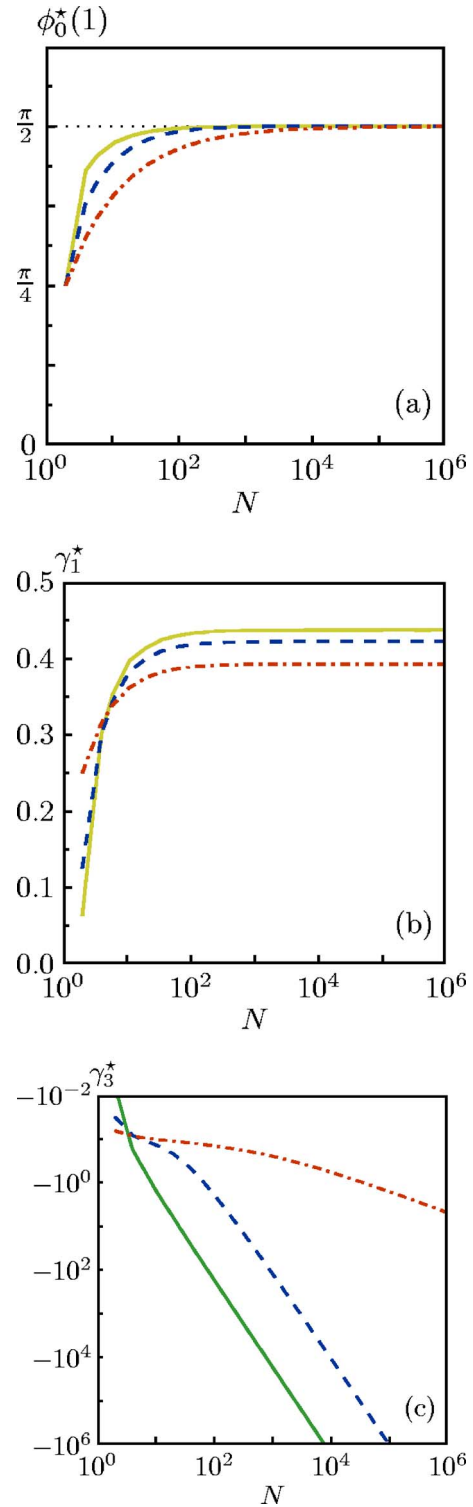


FIG. 4. (Color online) Scaling laws for discrete tentlike distributions. The curves show the N dependence of (a) $\phi_0^*(1)$, (b) γ_1^* , and (c) γ_3^* . The curves in panel (a) and (b) are shown for $h_0=1/2$ (dashed-dotted), $h_0=3/4$ (dashed), and $h_0=1$ (solid). In (c), γ_3^* is shown for values of $h_0=1/2$ (dashed-dotted, the limiting case of a discrete uniform distribution, which shows much weaker divergence than all the other curves), $h_0=3/4$ (dashed, a typical piecewise-linear distribution, which shows N^2 divergence), and $h_0=0.95$ (solid).

ACKNOWLEDGMENTS

Research of one of the authors (S.H.S.) was supported in part by National Science Foundation Grant No. DMS-0412757. The authors thank Joel Ariaratnam for sharing his initial work on this project, including the discovery of the

singular behavior discussed here. Nick Trefethen provided helpful guidance to the literature about quadrature rules near integrable singularities, and showed the authors how to improve the estimate of the constant c by using Richardson extrapolation.

-
- [1] A. T. Winfree, *J. Theor. Biol.* **16**, 15 (1967).
 [2] A. T. Winfree, *The Geometry of Biological Time* (Springer-Verlag, New York, 1980).
 [3] Y. Kuramoto, *Chemical Oscillations, Waves, and Turbulence* (Springer-Verlag, Berlin, 1984).
 [4] A. Pikovsky, M. Rosenblum, and J. Kurths, *Synchronization: A Universal Concept in Nonlinear Science* (Cambridge University Press, New York, 2001).
 [5] S. H. Strogatz, *Sync: The Emerging Science of Spontaneous Order* (Hyperion, New York, 2003).
 [6] S. C. Manrubia, A. S. Mikhailov, and D. H. Zanette, *Emergence of Dynamical Order: Synchronization Phenomena in Complex Systems* (World Scientific, Singapore, 2004).
 [7] L. Fabiny, P. Colet, R. Roy, and D. Lenstra, *Phys. Rev. A* **47**, 4287 (1993).
 [8] G. Kozyreff, A. G. Vladimirov, and P. Mandel, *Phys. Rev. Lett.* **85**, 3809 (2000).
 [9] M. Bennett, M. F. Schatz, H. Rockwood, and K. Wiesenfeld, *Proc. R. Soc. London, Ser. A* **458**, 563 (2002).
 [10] K. Wiesenfeld, P. Colet, and S. H. Strogatz, *Phys. Rev. Lett.* **76**, 404 (1996).
 [11] G. Filatrella, N. F. Pedersen, and K. Wiesenfeld, *Phys. Rev. E* **61**, 2513 (2000).
 [12] M. C. Cross, A. Zumdick, R. Lifshitz, and J. L. Rogers, *Phys. Rev. Lett.* **93**, 224101 (2004).
 [13] S. Kaka, M. R. Pufall, W. H. Rippard, T. J. Silva, S. E. Russek, and J. A. Katine, *Nature (London)* **437**, 389 (2005).
 [14] J. Buck, *Q. Rev. Biol.* **63**, 295 (1988).
 [15] T. J. Walker, *Science* **166**, 891 (1969).
 [16] E. Sismondo, *Science* **249**, 55 (1990).
 [17] W. Singer, *Annu. Rev. Physiol.* **55**, 349 (1993).
 [18] C. van Vreeswijk, L. F. Abbott, and G. B. Ermentrout, *J. Comput. Neurosci.* **1**, 313 (1994).
 [19] A. V. M. Herz and J. J. Hopfield, *Phys. Rev. Lett.* **75**, 1222 (1995).
 [20] W. Gerstner, J. L. van Hemmen, and J. D. Cowan, *Neural Comput.* **8**, 1653 (1996).
 [21] P. C. Bressloff and S. Coombes, *Phys. Rev. Lett.* **81**, 2168 (1998).
 [22] C. C. Chow, *Physica D* **118**, 343 (1998).
 [23] A. J. Preyer and R. J. Butera, *Phys. Rev. Lett.* **95**, 138103 (2005).
 [24] D. Golomb and D. Hansel, *Neural Comput.* **12**, 1095 (2000).
 [25] C. S. Peskin, *Mathematical Aspects of Heart Physiology* (Courant Institute of Mathematical Sciences, New York, 1975).
 [26] D. C. Michaels, E. P. Matyas, and J. Jalife, *Circ. Res.* **61**, 704 (1987).
 [27] S. Dano, P. G. Sorensen, and F. Hynne, *Nature (London)* **402**, 320 (1999).
 [28] M. K. McClintock, *Nature (London)* **229**, 244 (1971).
 [29] M. K. McClintock, *Annu. Rev. Sex Res.* **9**, 77 (1998).
 [30] Z. Neda, E. Ravasz, Y. Brechet, T. Vicsek, and A. L. Barabasi, *Nature (London)* **403**, 849 (2000).
 [31] S. H. Strogatz, D. M. Abrams, A. McRobie, B. Eckhardt, and E. Ott, *Nature (London)* **438**, 43 (2005).
 [32] Y. Kuramoto, in *International Symposium on Mathematical Problems in Theoretical Physics*, edited by H. Araki, Vol. 39 of *Lecture Notes in Physics* (Springer, Berlin, 1975), pp. 420–422.
 [33] G. B. Ermentrout, *J. Math. Biol.* **22**, 1 (1985).
 [34] Y. Kuramoto and I. Nishikawa, *J. Stat. Phys.* **49**, 569 (1987).
 [35] S. H. Strogatz and R. E. Mirollo, *J. Stat. Phys.* **63**, 613 (1991).
 [36] L. L. Bonilla, J. C. Neu, and R. Spigler, *J. Stat. Phys.* **67**, 313 (1992).
 [37] H. Daido, *Phys. Rev. Lett.* **73**, 760 (1994).
 [38] J. D. Crawford, *J. Stat. Phys.* **74**, 1047 (1994).
 [39] S. H. Strogatz, *Physica D* **143**, 1 (2000).
 [40] J. A. Acebrón, L. L. Bonilla, C. J. P. Vicente, F. Ritort, and R. Spigler, *Rev. Mod. Phys.* **77**, 137 (2005).
 [41] J. T. Ariaratnam and S. H. Strogatz, *Phys. Rev. Lett.* **86**, 4278 (2001).
 [42] R. Grimshaw, *Nonlinear Ordinary Differential Equations* (Blackwell, Oxford, 1990).
 [43] A. T. Winfree, *Science* **298**, 2336 (2002).
 [44] I. Z. Kiss, Y. Zhai, and J. L. Hudson, *Science* **296**, 1676 (2002).
 [45] D. Aeyels and J. A. Rogge, *Prog. Theor. Phys.* **112**, 921 (2004).
 [46] R. E. Mirollo and S. H. Strogatz, *Physica D* **205**, 249 (2005).
 [47] J. N. Lyness and B. W. Ninham, *Math. Comput.* **21**, 162 (1967).
 [48] B. W. Ninham and J. N. Lyness, *Math. Comput.* **23**, 71 (1969).